Lattice optimization for the HLS-Ⅱ storage ring*

BAI Zheng-He(白正贺)[1)] WANG Lin(王琳)[2)] JIA Qi-Ka(贾启卡) LI Wei-Min(李为民)

National Synchrotron Radiation Laboratory, University of Science and Technology of China, Hefei 230029, China

Abstract: The upgrade project of the Hefei Light Source (HLS), named HLS-Ⅱ, is under way, which includes the reconstruction of its storage ring. The HLS-Ⅱ storage ring has lower emittance and more straight sections available for insertion devices as compared with the present HLS storage ring. The scan method is applied to the linear lattice optimization for the HLS-Ⅱ storage ring to get thorough information about the lattice. To reduce the amount of computation, several scans with different grid spacing values are conducted. In addition, the calculation of the chromatic sextupole strength for the achromatic mode is included in the scan, which is useful for nonlinear lattice optimization. To better analyze the obtained solutions in the scan, the lattice properties and the variables of quadrupole strengths are statistically analyzed. The process of selecting solutions is described in detail, including the choice of the working point, the settings for the emittance and optical functions, and the restriction of maximum magnet strength. Two obtained lattices, one for the achromatic mode and the other for the non-achromatic mode, are presented, including their optical functions and optimized dynamic apertures.

Key words: storage ring, lattice, scan, optimization, emittance, dynamic aperture

PACS: 29.20.db, 29.27.Bd **DOI:** 10.1088/1674-1137/37/1/017001

1 Introduction

The Hefei Light Source (HLS) at National Synchrotron Radiation Laboratory, which is a second generation dedicated VUV and soft X-ray synchrotron radiation light source, has been in operation for over 20 years. The HLS is composed of a 200 MeV injector linac, a beam transfer line, and an 800 MeV storage ring. The storage ring consists of 4 identical TBA cells, with an emittance of 166 nm·rad and a circumference of about 66 m.

Many low emittance synchrotron radiation light sources have been built around the world for providing high brightness photon beams for synchrotron radiation experiments. To obtain lower emittance, some existing light sources are upgrading their facilities, such as the Advanced Light Source (ALS). A proposal for upgrading the HLS was submitted two years ago to enhance the competitiveness of the HLS. The upgraded light source, named HLS-Ⅱ, would have lower emittance and more insertion devices.

The energy and circumference of the HLS-Ⅱ storage ring are the same as those of the HLS. The HLS-Ⅱ storage ring contains 8 dipoles, forming 4 identical DBA cells in the achromatic mode with an emittance of less than 40 nm·rad. In the non-achromatic mode, the emittance is about 20 nm·rad. Compared with the HLS, the emittance of HLS-Ⅱ is reduced by about half an order of magnitude in the achromatic mode. In addition, more straight sections are available for insertion devices in the HLS-Ⅱ storage ring. After reconstruction, the HLS-Ⅱ will have better performance than similar machines around the world.

The HLS-Ⅱ storage ring lattice has a simple structure with several tunable parameters, where the parameters are the magnet strengths used for lattice optimization. So, naturally, the scan method [1] is applied to the linear lattice optimization for the HLS-Ⅱ storage ring. The scan method can provide the global information about the lattice, which is very helpful for lattice studies. The data post-processing is indispensable for dealing with the database that is obtained through the scan method. Then one can select the required information from the database.

In the HLS-Ⅱ storage ring lattice, there are four variables of quadrupole strengths. So, in our case, to reduce the amount of computation, several scans with different grid spacing values have been conducted. In the achromatic mode, there are two families of chromatic sextupoles used to compensate the horizontal and verti-

Received 20 February 2012

∗ Supported by National Natural Science Foundation of China (11175182, 10979045)

1) E-mail: baizheng@mail.ustc.edu.cn

2) E-mail: wanglin@ustc.edu.cn

cal natural chromaticities. That means that the strengths of the two chromatic sextupoles can be determined. So the calculation of these two chromatic sextupole strengths is included in our scan, which is useful for the next nonlinear optimization. To better analyze the selected solutions from the obtained database, the properties of the lattice and the variables of quadrupole strengths are statistically analyzed in the data post-processing. This statistical analysis is convenient for the lattice study.

In this paper we study the overall linear properties of the HLS-Ⅱ storage ring lattice, and describe the detailed process of selecting valuable solutions from the obtained data in the scan. Then two solutions, one for the achromatic mode and the other for the non-achromatic mode, are selected as candidate lattices, and their optical functions and optimized dynamic apertures are presented in this paper.

2 Storage ring lattice optimization

The HLS-Ⅱ storage ring lattice has a DBA structure with 4 periods in the achromatic mode, and the magnet layout of one period is schematically shown in Fig. 1. There are four families of quadrupoles (Q1, Q2, Q3 and Q4) and four families of sextupoles (S1, S2, S3 and S4) in the lattice. There is a 4 m long straight section (DL) and a 2.3 m medium straight section (DM) in each period, providing space for injection, RF cavity and insertion devices.

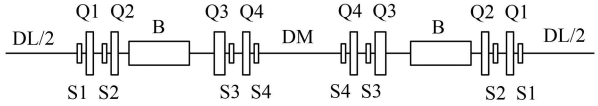

Fig. 1. The magnet layout of one period of the HLS-Ⅱ storage ring.

2.1 Scan method and results

Usually, accelerator designers tune the lattice to obtain as many desired lattice properties as possible through trial and error using some professional codes for accelerator design. In recent years, the scan method and artificial intelligence algorithms (like genetic algorithms and particle swarm optimization) have been applied to assist designers in linear and nonlinear lattice design and optimization. In linear lattice optimization, artificial intelligence algorithms can solve problems with more than three or four variables well, where the scan method cannot be applied due to the huge amount of computation. Considering that there are four variables of quadrupole strengths, and that the scan method can give us thorough information about the lattice, we think that the scan method is the best choice in the linear lattice optimization for the HLS-Ⅱ storage ring.

For independence and future plan, we wrote the code for calculating lattice properties. No other accelerator design code is used in our scan. The HLS-Ⅱ storage ring is a small ring with a small curvature radius, so the dipole contribution to the natural chromaticities is very important and cannot be neglected. In our code, the calculation of the natural chromaticities has been carefully considered according to the formula in Ref. [2]. Additionally, the dipole fringe field has an important effect on the calculation of vertical beta function and vertical tune. The value of the dipole fringe field integral is set to 0.625 according to the present magnet design.

To reduce the computation amount in our scan, we first scan the whole variable space with larger grid spacing to obtain rough information about the lattice, and then scan the selected regions of interest with smaller grid spacing values to obtain detailed information.

So, first, the strengths of the four quadrupole families are scanned in the large range [-10 m^{-2}, 10 m^{-2}] with a grid spacing of 0.1 m^{-2}. There are about 1.6 billion quadrupole strength points scanned in total. If one point is a stable solution, its associated lattice properties are calculated in the scan. In this scan, the calculation of lattice properties includes the natural emittance, the Twiss parameters, and the dispersion function at some specific points (such as the middle points of long straight section DL and medium straight section DM), the maximum values of beta functions and the maximum absolute value of dispersion in the lattice, the working point (including the betatron phase advances over one period), and the momentum compaction factor.

We set some basic requirements for the natural emittance ε_x, horizontal beta function β_x and vertical beta function β_y to select solutions:

(1) $\varepsilon_x < 40$ nm·rad;

(2) maximum β_x, β_y <25 m;

(3) β_x at the center of DL >5 m;

(4) β_y at the center of DL <5 m.

After the scan, there are about 5.5 thousand solutions satisfying the above basic requirements. The strengths of quadrupole Q1 for all these solutions are all larger than zero (i.e., the focusing quadrupole), and the strengths of Q2 are all less than zero (i.e., the defocusing quadrupole). But the quadruples Q3 and Q4 can be focusing or defocusing. For most of these solutions, about 94 percent, the quadrupole Q3 is focusing and Q4 is defocusing. For the other 6 percent of solutions, we have made the statistical analysis including the calculation of maximum, minimum and average values of lattice properties. We found that among the 6 percent of solutions there is no achromatic-mode solution due to large dispersion at the center of DL, and that the minimum emittance is larger relative to that in the region where Q3 is focusing and

Q4 is defocusing.

Our study focuses on the region where Q3 is focusing and Q4 is defocusing. Then we scan this region of interest with a smaller grid spacing of 0.02 m^{-2}. Besides the calculation of the lattice properties mentioned above, considering the next nonlinear optimization, some other calculations are included in this scan.

In order to correct the natural chromaticities, sextupole magnets are employed, which introduce significant nonlinearities into the lattice limiting the dynamic aperture. In the lattice design, to reduce the sextupole strength, it is hoped that the natural chromaticities can be relatively small, and that the horizontal and vertical beta functions can be well separated and the dispersion can be large at the sextupole location. In the achromatic mode of the HLS-Ⅱ storage ring lattice, there are only two families of sextupoles, S3 and S4, used to correct the horizontal and vertical natural chromaticities. So, given the values of the dispersion and beta functions at the sextupole location and, the natural chromaticities and corrected chromaticities, the strengths of the two families of chromatic sextupoles can be calculated and only determined. Of course, we will not choose the solution which has large sextupole strength beyond the maximum design value of sextupole strength, even if the lattice properties of the solution are satisfactory. Additionally, too strong sextupole magnets may result in a relatively small dynamic aperture.

In this scan, the additional calculation includes the natural chromaticities and the strengths of the two chromatic sextupoles, S3 and S4, used to correct the natural chromaticities to zero. After this scan, there are about 3 million solutions satisfying the basic requirements mentioned above. These obtained solutions are in two regions, A and B, which can be seen in the strength space of the quadrupoles, Q2 and Q4, as shown in the right plot of Fig. 2. Of the 3 million solutions, about one-tenth of the solutions are in region B. Most of the solutions are in region A.

With the function of minimum value in our statistical analysis, we have compared the lowest emittances obtained in the two scans respectively with the grid spacing values of 0.1 m^{-2} and 0.02 m^{-2}. For the achromatic mode of the HLS-Ⅱ storage ring, the minimum emittance is 27.8 nm·rad with J_x=1.055 according to the following formula:

$$\varepsilon_{\rm MEDBA} = \frac{C_{\rm q}\gamma^2\theta^3}{4\sqrt{15}J_x}, \tag{1}$$

where $C_{\rm q}=3.83\times10^{-13}$ m, γ is the relativistic factor, θ is the dipole bending angle, and J_x is the horizontal damping partition number. For the obtained solutions in the scan, we consider the solution that has the absolute value of dispersion at the center of DL, $|\eta_0|$, less than a specified value to be achromatic. From Table 1, we can see that, if the specified value is not very small, $|\eta_0|<0.1$ m, the two lowest emittances, 25.9 nm·rad and 25.6 nm·rad, obtained in the two scans are close. If we set the specified value to be smaller, for example, $|\eta_0|<0.05$ m or $|\eta_0|<0.02$ m, the difference between the two scans becomes obvious. We can also see that in the condition of $|\eta_0|<0.02$ m for the achromatic mode, the obtained lowest emittance in the scan with the grid spacing value of 0.02 m^{-2}, 28.1 nm·rad, is close to the minimum emittance of 27.8 nm·rad.

For the non-achromatic mode, the minimum emittance is 9.3 nm·rad with J_x=1.055 according to the formula:

$$\varepsilon_{\rm TME} = \frac{1}{3}\varepsilon_{\rm MEDBA} = \frac{C_{\rm q}\gamma^2\theta^3}{12\sqrt{15}J_x}. \tag{2}$$

From Table 1, we can see that the two lowest emittances,

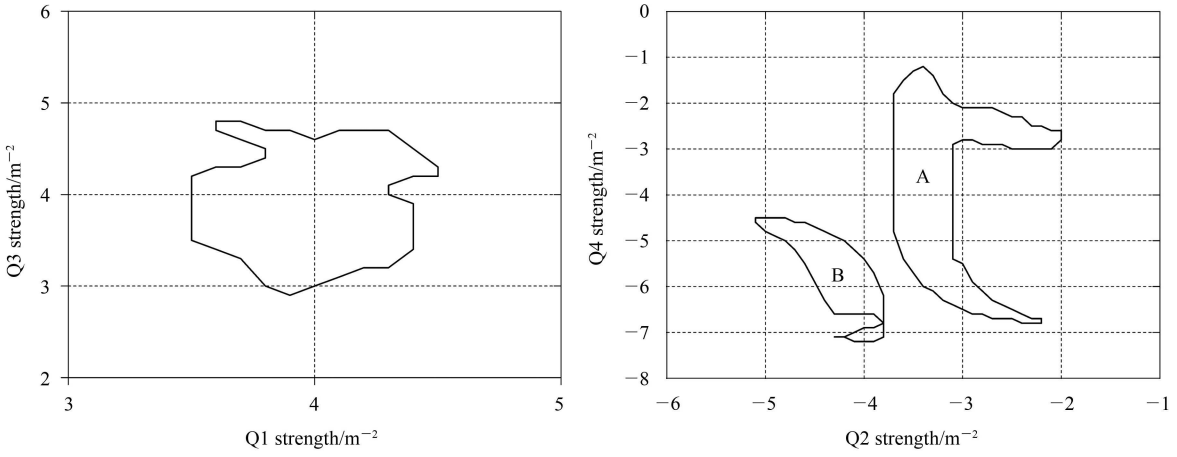

Fig. 2. The strength regions of the quadrupoles Q1, Q3 (the left plot) and Q2, Q4 (the right plot) having the solutions satisfying the basic requirements.

Table 1. The comparison of the lowest emittances obtained in the two scans respectively with the grid spacing values of 0.1 m^{-2} and 0.02 m^{-2}.

	achromatic mode				non-achromatic mode			
	minimum emittance (J_x=1.055)	lowest emittance with $\|\eta_0\|$ <0.1 m	lowest emittance with $\|\eta_0\|$ <0.05 m	lowest emittance with $\|\eta_0\|$ <0.02 m	minimum emittance (J_x=1.055)	lowest emittance	number in [14, 14.5] nm·rad	number in [14, 15] nm·rad
scan with 0.1 m^{-2}	27.8 nm·rad	25.9 nm·rad	29.4 nm·rad	29.8 nm·rad	9.3 nm·rad	14.1 nm·rad	58	257
scan with 0.02 m^{-2}	27.8 nm·rad	25.6 nm·rad	27.1 nm·rad	28.1 nm·rad	9.3 nm·rad	14.0 nm·rad	49255 (≈850×58)	167480 (≈650×257)

14.1 nm·rad and 14.0 nm·rad, obtained in the two scans are almost the same, which are, however, not close to the minimum emittance of 9.3 nm·rad. Compared with the scan with the grid spacing value of 0.1 m^{-2}, the density of the solutions obtained in the scan with 0.02 m^{-2} can be increased 625 times (5×5×5×5). We can also see that the number of solutions in the range [14 nm·rad, 14.5 nm·rad] obtained in the scan with 0.02 m^{-2} is about 850 times that in the scan with 0.1 m^{-2}. If we relax the range to [14 nm·rad, 15 nm·rad], it is about 650 times, which is close to the number of 625. Table 1 tells us that the difference between the data obtained in the two scans becomes obvious when some constraints are strict, which is also easy to understand. It also tells us that, the HLS-Ⅱ storage ring has the potential to reach such low emittance.

But in fact, the emittances of the lattices selected as the candidates for the HLS-II storage ring are higher than the above lowest emittances. That is to say, we have not chosen the lattices with such low emittances. This is because, in addition to the basic requirements mentioned above, there are many other restrictions to be considered, such as the choice of the working point, the restriction of maximum magnet strength and the consideration of nonlinear dynamics. In the following text, we will discuss these issues.

2.2 Solution selection and lattice optimization

According to the magnet design for the HLS-Ⅱ storage ring [3], the quadrupole strength is required to be less than 5 m^{-2}, and the sextupole strength is less than 120 m^{-3}.

For most of the solutions in region B shown in Fig. 2, the strength of the quadrupole Q4 is larger than the maximum strength value of 5 m^{-2}. In addition, we have made the statistical analysis for the solutions in region B, and the minimum β_x at the center of DL is 14.3 m. That is to say, the solutions in region B have a common characteristic of large β_x at the center of DL.

Next, we will study the solutions in region A shown in Fig. 2. Our study focuses on the upper part of region A, where the solutions have the strength of the quadrupole Q4 less than 5 m^{-2}. In the data post-processing, we set strict requirements to further select the solutions with more satisfactory and detailed parameters.

Concerning the working point, it should be away from the integer and half-integer values to reduce the sensitivity of some distortions to dipole and quadrupole field errors, and it should be also away from destructive resonances. The number of superperiods of the HLS-Ⅱ storage ring is 4. In the real world, due to imperfections and perturbations, strictly speaking, there is only one superperiod, which is the ring itself. The imperfections and perturbations break the periodicity of the ring to some extent, which will cause the excitation of some resonances that are not allowed in the ideal situation of perfect periodicity, reducing the dynamic aperture [4]. So in our solution selection process, the working point is required to be away from the third-order resonances driven by normal sextuples, even if the resonances are unallowed in the ideal situation. The working point is also away from the second-order coupling resonances. The structural resonances are carefully considered, including higher-order structural resonances. Actually, for the HLS-Ⅱ storage ring, we found that the fifth-order structural resonances have an important effect on nonlinear dynamics in our nonlinear optimization. Moreover, we hope that the fractional parts of the tunes can be below 0.5 to control the resistive wall instability.

Detailed above are the requirements for the choice of the working point. Next we set more stringent requirements for the emittance and optical functions. For the achromatic mode, we set the natural emittance ε_x to be less than 36 nm·rad. The value of β_x at the center of DL is set to be larger than 10 m for injection. To obtain high brightness, β_y at the center of DL is less than 3 m, and β_x and β_y at the center of DM are less than 5 m and 3 m, respectively. The maximum absolute value of dispersion is less than 1.5 m. And, the absolute value of dispersion at the center of DL is less than 0.05 m, which we consider the condition of being achromatic in the case of scanning with the grid spacing of 0.02 m^{-2}.

Moreover, all the four quadrupole strengths are set to be less than the maximum value of 5 m^{-2}. For the

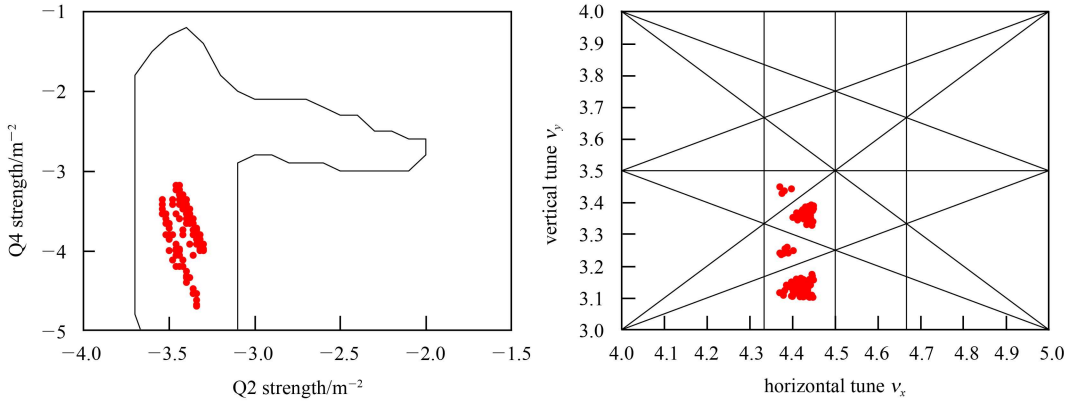

Fig. 3. (color online) The selected solutions (the red dots) for the achromatic mode shown in the strength space of the quadrupoles Q2 and Q4 (the left plot) where the shape of the upper part of region A is plotted, and in the tune space (the right plot) where the resonance lines up to the third order are plotted.

achromatic mode, the strengths of the two chromatic sextpuoles S3 and S4 are set to be less than the maximum value of 120 m^{-3}.

In our data post-processing, the solutions satisfying the strict requirements mentioned above can be picked out. But in this solution selection, the structural resonances of the fourth or higher order are not considered in selecting the working point. Because we think the grid spacing of 0.02 m^{-2} is not small enough. After this selection, some more satisfactory solutions are obtained. In fact, there are about 100 such selected solutions in total, and they are shown in the strength space of quadrupoles Q2 and Q4 in the left plot of Fig. 3 (the red dots). We also show them in the tune space in the right plot of Fig. 3 (the red dots), where we can see that these solutions are away from the resonance lines up to the third order and that the fractional parts of the tunes of these solutions are below 0.5. For these obtained solutions, not only their lattice properties but also their quadrupole strengths are statistically analyzed. The statistical analysis of quadrupole strength includes the calculation of maximum, minimum and average values of the strengths of the four families of quadrupoles. From the maximum and minimum values of the quadrupole strengths, we can get the range of the quadrupole strengths of these solutions. That is to say, we can get the region where these solutions are located. For example, the strength range of the quadrupole Q2 is [−3.54 m^{-2}, −3.30 m^{-2}], and the range of Q4 is [−4.70 m^{-2}, −3.18 m^{-2}].

Then we scan this small region with an even smaller grid spacing of 0.005 m^{-2}, which is small enough to obtain more solutions with more detailed information. Compared with the spacing of 0.02 m^{-2}, the density of solutions is increased 256 times (4×4×4×4). This mainly brings two advantages. First, we can set a stricter condition of being achromatic, i.e., the absolute value of dispersion at the center of DL is less than, for example, 0.002 m. Secondly, because the density of solutions in tune space is higher, we can better consider higher order structural resonances in selecting the working point.

Eventually, we obtained some candidate solutions for the achromatic mode through such scans and strict selection. For the achromatic mode, the strengths of chromatic sextupoles are also obtained. So we can directly examine the dynamic aperture using some widely used accelerator design codes. In addition to sextupoles S3 and S4, there are two families of sextupoles, S1 and S2, at the dispersion-free DL straight section that can be used as harmonic sextupoles to control the geometrical aberrations to improve the dynamic aperture. In fact, we found that the two families of harmonic sextupoles can well control the amplitude dependent tune shift in our nonlinear optimization. So here we include sextupoles S1 and S2 in the nonlinear optimization.

Compared with the calculation of linear parameters, the calculation of the dynamic aperture consumes much time. So artificial intelligence algorithms are naturally considered to optimize the strengths of sextupoles S1 and S2 to improve the dynamic aperture. Here we use the particle swarm optimization (PSO) algorithm [5], which is a widely used artificial intelligence algorithm. We have successfully applied the PSO algorithm to the dynamic aperture optimization for other lattices [6]. For more details about this application, one can refer to Ref. [6]. With frequency map analysis (FMA), we can choose and slightly tune the optimization results to refine the quality of the dynamic aperture after dynamic aperture optimization. Also, the FMA can direct the working point selection from those solutions in the vicinity of the studied solution. Because there are only two families of harmonic sextupoles to be optimized, the scan method can also be used to optimize the harmonic sextupoles to improve the dynamic aperture, and then the FMA is used to choose and analyze the optimization results, as the

AS had done [7]. In our nonlinear optimization, we used the Elegant [8] code for tracking.

Finally, we can obtain some solutions for the achromatic mode having satisfactory linear lattice properties and good nonlinear performance. Here we show one obtained solution for the achromatic mode. Its lattice optical functions of one period are shown in Fig. 4, and the on- and off-momentum dynamic apertures are shown in Fig. 5. The dynamic apertures are tracked with the physical aperture of x=38 mm and y=10 mm. In fact, the dynamic apertures without physical aperture limitation are larger than the physical aperture. The natural emittance is 34.6 nm·rad, and the working point is (4.380, 3.145). The values of β_x and β_y at the center of DL are, respectively, 20.62 m and 2.40 m, and β_x and β_y at the center of DM are, respectively, 3.66 m and 1.82 m. The momentum compaction factor is 0.0205.

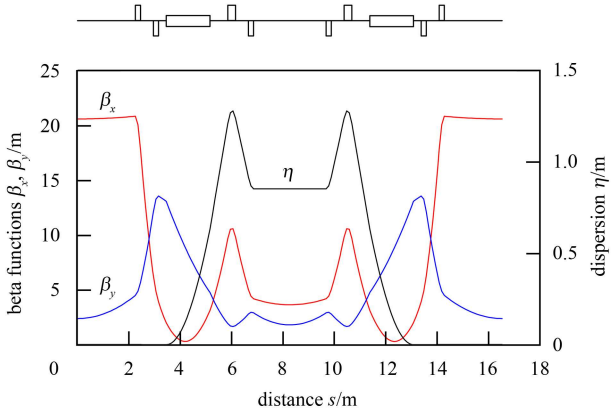

Fig. 4. (color online) The optical functions of one period for the achromatic mode.

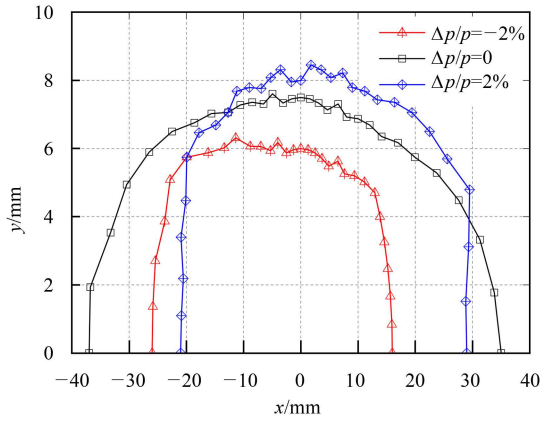

Fig. 5. (color online) The on- and off-momentum dynamic apertures for the achromatic mode (tracked with the physical aperture).

For the non-achromatic mode, some settings for solution selection are different from those for the achromatic mode. First, there is not the requirement that the dispersion at the center of DL is near zero, but the dispersion at the center of DL is set to be less than 0.8 m. Secondly, the natural emittance is set to be less than 20 nm·rad. Thirdly, the calculation results of the strengths of the sextupoles S3 and S4 are not suitable for the non-achromatic mode, because there are four families of chromatic sextupoles, S1, S2, S3, and S4, used to compensate the natural chromaticities. All the other settings are the same as those in the achromatic mode.

In the nonlinear optimization for the non-achromatic mode, the PSO algorithm is also used to optimize the strengths of sextupoles S1, S2, S3, and S4 to enlarge the dynamic aperture, and the natural chromaticities are corrected to zero. The optical functions of one obtained solution are shown in Fig. 6, and Fig. 7 shows the corresponding on- and off-momentum dynamic apertures. We can see that the off-momentum dynamic apertures are reduced compared with those in the achromatic mode shown in Fig. 5. This is due to the large dispersion at the center of DL, and the dynamic apertures without physical aperture limitation are also larger than the physical

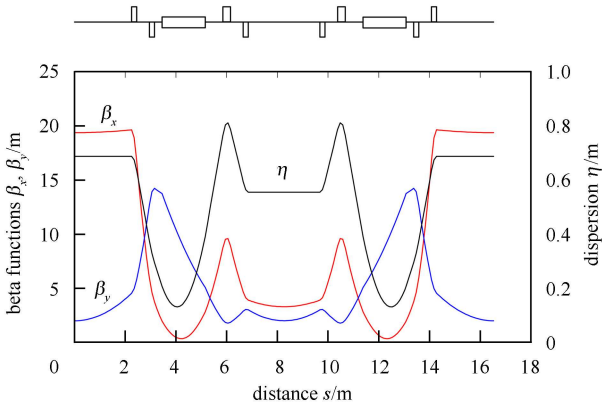

Fig. 6. (color online) The optical functions of one period for the non-achromatic mode.

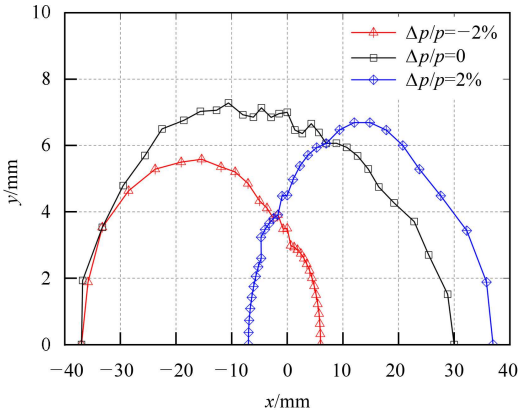

Fig. 7. (color online) The on- and off-momentum dynamic apertures for the non-achromatic mode (tracked with the physical aperture).

aperture. The natural emittance is 19.8 nm·rad, and the working point is (4.414, 3.147). The values of β_x and β_y at the center of DL are 19.37 m and 1.99 m, respectively, and β_x and β_y at the center of DM are respectively 3.28 m and 1.99 m. The momentum compaction factor is 0.0187.

We can change the restriction in the solution selection to find interesting solutions from the obtained data. It is obvious that our work is very helpful for the future lattice study of the HLS Ⅱ storage ring.

3 Conclusion

We have applied the scan method to the lattice optimization for the HLS II storage ring, and several scans with different grid spacing values are conducted to reduce the computation amount. In our scan, the lattice properties and the variables of quadrupole strengths can be statistically analyzed for the obtained solutions to better understand the overall situation about the solutions. To make the obtained solutions more feasible in practice, strict solution selection is conducted, including the choice of the working point, the settings for the emittance and optical functions, and the restriction of maximum magnet strength. In addition to the calculation of lattice properties, we especially include the calculation of the strengths of two chromatic sextupoles used to compensate the natural chromaticities in the achromatic mode in our scan, which is useful for nonlinear optimization. Finally, two solutions are selected as the candidate lattices respectively for the achromatic mode and the non-achromatic mode. They not only have good linear lattice properties, but also large optimized on- and off-momentum dynamic apertures.

We are now considering the inclusion of the calculation of other parameters of merit, such as the insertion device brightness and some nonlinear quantities, in our scan to make our program more powerful. If so, we can take the brightness as the optimization goal. Obviously, the work we present here is not limited to the lattice optimization for the HLS II storage ring, and it can also be suitable for other lattices with simple structures or fewer variables.

References

1 David S Robin, WAN Wei-Shi, Fernando Sannibale. Phys. Rev. ST Accel. Beams, 2008, **11**(2): 024002

2 Hardt W, Jager J, Mohl D. A General Analytical Expression for the Chromaticity of Accelerator Rings. CERN PS/LEA/Note 82-5, 1982

3 ZHANG Hao, LI Wei-Min, FENG Guang-Yao et al. Chin. Phys. C (HEP & NP), 2012, **36**(1): 91

4 Robin D, Safranek J, Decking W. Phys. Rev. ST Accel. Beams, 1999, **2**(4): 044001

5 James Kennedy, Russell Eberhart. Particle Swarm Optimization. In: Proc. IEEE Int'l. Conf. on Neural Networks. Piscataway, NJ: IEEE Service Center, 1995. 1942

6 BAI Zheng-He, WANG Lin, LI Wei-Min. Enlarging Dynamic and Momentum Aperture by Particle Swarm Optimization. In: Proc. of IPAC 2011. Spain: San Sebastian, 2011. 948

7 Tan Y R E, Boland M J, LeBlanc G. Applying Frequency Map Analysis to the Australian Synchrotron Storage Ring. In: Proc. of 2005 PAC. USA: Knoxville, 2005. 407

8 Borland M. Elegant: A Flexible SDDS-Compliant Code for Accelerator Simulation. APS LS-287, 2000